A Computational Model of Electrical Stimulation of the Retinal Ganglion Cell

Robert J. Greenberg,* *Member, IEEE,* Toby J. Velte, Mark S. Humayun, George N. Scarlatis, and Eugene de Juan, Jr.

***Abstract*—Localized retinal electrical stimulation in blind volunteers results in discrete round visual percepts corresponding to the location of the stimulating electrode. The success of such an approach to provide useful vision depends on elucidating the neuronal target of surface electrical stimulation. To determine if electrodes preferentially stimulate ganglion cells directly below them or passing fibers from distant ganglion cells, we developed a compartmental model for electric field stimulation of the retinal ganglion cell (RGC). In this model a RGC is stimulated by extracellular electrical fields with active channels and realistic cell morphology derived directly from a neuronal tracing. Three membrane models were applied: a linear passive model, a Hodgkin–Huxley model with passive dendrites (HH), and a model composed of all active compartments (FCM) with five nonlinear ion channels. Idealized monopolar point and disk stimulating electrodes were positioned above the cell. For the HH and FCM models, the position of lowest cathodal threshold to propagate an action potential was over the soma. Brief (100 μs) cathodic stimuli were 20% (HH with disk electrode) to 73% (FCM with point-source) more effective over the soma than over the axon. In the passive model, the axon is preferentially stimulated versus the soma. Although it may be possible to electrically stimulate RGC's near their cell body at lower thresholds than at their axon, these differences are relatively small. Alternative explanations should be sought to explain the focal perceptions observed in previously reported patient trials.**

***Index Terms*— Amphibian, extracellular fields, ganglion cell, human, modeling, retina, visual prosthesis.**

I. Introduction

RECENTLY, an intraocular prosthesis which would electrically stimulate surviving retinal ganglion cells (RGC's) in patients blind from photoreceptor degeneration has been proposed [1]–[3]. There are 1.2 million people worldwide with photoreceptor degeneration diseases such as retinitis pigmentosa (RP) [4]. There is also some evidence that such a prosthesis might also benefit patients with severe age-related macular degeneration (AMD) [5], which is the leading cause of blindness in Western countries. Although these patients are blind, they possess functioning ganglion cells which relay retinal input to the brain [6]–[10].

Manuscript received July 19, 1996; revised January 6, 1999. The work of R. J. Greenberg and E. de Juan, Jr. was supported in part by a grant from the Jaffe Family Foundation. This work was supported by the Whitaker and Grousbeck Family Foundations. *Asterisk indicates corresponding author.*

*R. J. Greenberg is with the Department of Biomedical Engineering, The Johns Hopkins University, Baltimore, MD 21205 USA (e-mail: bob@jhu.edu). He is also with the Wilmer Eye Institute, Johns Hopkins Hospital, Baltimore, MD 21287 USA.

T. J. Velte is with the Howard Hughes Medical Institute, Harvard Medical School, Boston, MA 02114 USA.

M. S. Humayun, G. N. Scarlatis, and E. de Juan, Jr. are with The Wilmer Eye Institute, Johns Hopkins Hospital, Baltimore, MD 21287 USA.

Publisher Item Identifier S 0018-9294(99)03113-4.

We have previously shown that patients blind from RP resolve focal phosphenes when the ganglion cell side of the retinal surface is stimulated with 50- to 200-μm-diameter disk electrodes less than 500 μm apart [1]. None of these patients reported the perception of wedges: all reported spots of light or spots surrounded by dark rings.

This finding was significant, since at any particular location on the surface of the retina, axons from distant sites overlie the individual ganglion cell bodies. If these superficial passing fibers were preferentially stimulated by a prosthesis, groups of ganglion cells from large areas of the retina would be excited. One might expect the visual perception of such a stimulus to appear as a wedge (patients with selective losses of a ganglion cell axons at a focal location experience wedge-shaped visual field defects like the shape shown in Fig. 1(a) [11]. Moreover, since the visual world is mapped onto the surface of the retina such that the area of stimulated RGC's corresponds spatially to the visual image perceived, this response is logical. On the other hand, if the ganglion cells were stimulated near their cell bodies, we would expect the visual perceptions to be focal spots as seen in Fig. 1(b) (patients with focal ablation of the retina perceive a discrete scotoma or blind spot). Obviously, a prosthesis which produced discrete spots of perceived "light" would have a higher resolution and produce a better image than one which produced large wedges or streaks of perceived "light." It is also possible that the dendrites are preferentially stimulated [Fig. 1(c)]. Since the dendritic arbor of a single ganglion cell may spread up to 500 μm in diameter and overlap the dendritic field of other ganglion cells [12], stimulation of dendrites might lead to larger perceived spots than if the soma was preferentially stimulated.

To explore the relative thresholds of ganglion cell axons, somas, and dendrites, we have developed a computational model for electric field stimulation of the RGC. In the past, several models have been used to explore the response of isolated axons or somas (spheroidal shapes) to extrinsic electrical stimulation [13]. Most analytical models have represented the cell membrane as a resistor and capacitor in parallel (passive RC circuit). An excellent example of electrical stimulation of a passive model for unmyelinated axons was described by Rubinstein and Spelman [14]. More recently, Plonsey and Barr performed a numerical simulation including Hodgkin–Huxley active membrane properties, which they suggest may be a better predictor of axon response compared to passive approximations [15]. Despite a large body of material on axonal stimulation, to date, the only model of extrinsic electrical stimulation of an entire cell using morphology obtained directly from a real neuron was a passive

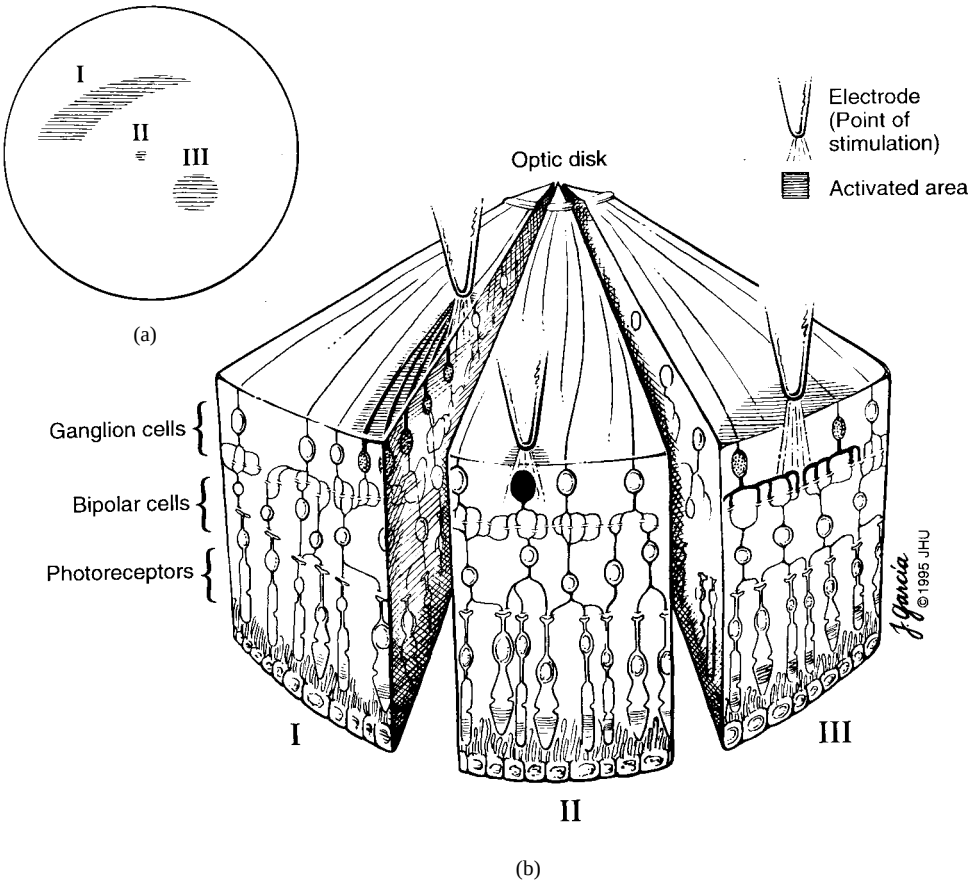

Fig. 1. Electrical stimulation of the retinal ganglion cell via its axon (I), soma (II), or dendrites (III): (a) visual fields which would be produced by stimulation of the retinal ganglion cell axon (I), soma (II), or dendrites (III) and (b) cross section of retina showing electrodes and activated ganglion cells. Ganglion cells are shown on the top surface while the bipolar cells and photoreceptors are below. The stimulating electrode is schematically represented above the ganglion cells.

model of cortical pyramidal cells analyzed by Hause in 1975 [16]. No models have studied an entire traced cell (i.e., cell body, axon, and dendrites) with active membrane properties.

To simulate electrical stimulation of the RGC, our approach was to map a representative RGC in three dimensions. We then divided the cell into compartments as described by Rall [17]. To these compartments, we applied the extracellular field of an ideal monopolar point or disk electrode in a homogeneous medium. Using NEURON [18], a multicompartmental simulation package, we tested three cell membrane models—a passive and two active models. Our simulations, we believe, are the first to model a neuron stimulated by extracellular electrical fields with active channels and realistic morphology derived directly from a neuronal tracing.

Our results suggest that there may be a lower threshold for stimulation at or near the RGC's cell body when compared with their axon. However, the results also show that these thresholds vary by less than a factor of two which may not be sufficient to form the sole explanation for the focal phosphenes observed.

II. Methods

A. Definitions

Cathodic is defined with respect to the vitreous monopolar electrode.

The *threshold response* (to the minimum stimulation current) for the passive model is defined traditionally as a 15 mV depolarization [13]. Threshold response for the active models are defined as initiation of an action potential which propagates down the axon.

The *initial site of excitation* is defined as the location on the cell where the membrane potential first crosses 0 mV on its way to produce an action potential (stimulus intensity at threshold).

B. Creation of the Model

1) Cell Tracing and Conversion to Electrical Network Model: An amphibian (mudpuppy—*Necturus maculosus*) ganglion cell was injected intracellularly with the tracer compound Neurobiotin (Vector Laboratories, Inc., Burlingame, CA) [19]. The retina was mounted and the ganglion cell was traced using the Eutectic Neuronal Tracing System (ENTS, Eutectic Electronics, Raleigh, NC [20], [21]). The X, Y, and Z coordinates of the dendrites and axon, along with their thickness and hierarchical structure, were recorded in an ASCII file which contained the intact three-dimensional structure of the soma, dendritic tree and axon. A shareware software utility called *ntscable* (written by Raimond Winslow), running on a Sun IPX workstation, was used to convert the ASCII file into a structure that was readable by the general neuronal simulator, NEURON Windows ver. 3.0 [18]. Neuron was written by

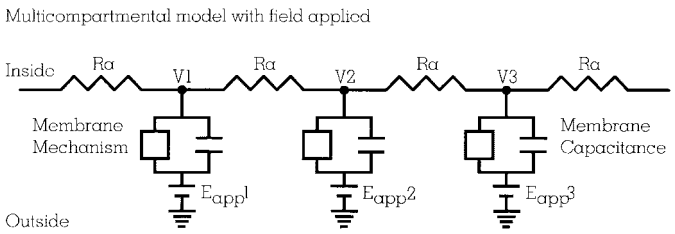

Fig. 2. Electrical circuit diagram representation of the retinal ganglion cell during and after the application of an extracellular stimulus. Three membrane mechanisms were modeled in parallel with a leak conductance which consisted of a battery in series with a conductance. The passive membrane mechanism consisted of a simple conductance. The two active membrane mechanisms consisted of variable conductances in series with batteries. The conductances were defined by the Hodgkin–Huxley formulations for each ionic channel. The batteries were defined by the corresponding reversal potential of the ion they represent.

Michael Hines and uses a fully implicit (backward Euler) method of integration.

To explore the influence of the dendritic and axonal cellular structure on the threshold, a cell with a large dendritic field and a long axon was chosen. We chose the "large cell" from [19, Fig. 1]. Note, the full extent of the axon is not shown in the Velte and Miller paper but was traced and is included in these simulations as can be seen in Figs. 3 and 4. Several constants were specified based on whole-cell recording data which included the value for membrane capacitance (1 μF/cm^2), membrane resistance (50 000 Ωcm^2) [22], and cytoplasmic resistance (110 Ωcm) [22]. These values are assumed to be uniform throughout the cell. Each compartment in the simulation was modeled as in Fig. 2. The simulations were modeled at room temperature (22°C). We chose to perform these simulations at 22°C so that the results could be compared to amphibian electrophysiological experiments which are carried out at room temperature. In addition, it is known that the Hodgkin–Huxley equations do not propagate action potentials above 31°C [23].

The soma is modeled as a compartmentalized sphere. The compartments lie parallel to the plane of the retina—as if sliced horizontally by an egg-slicer (i.e., a cable with varying diameters). A soma diameter of 24 μm was used for most simulations. This size was chosen to approximate the diameter of the actual traced mudpuppy soma. To examine the effect of soma size on threshold, a 10-μm-diameter soma was also used.

The dendrites and axon were all connected to the center compartment of the soma. The neuron was then segmented into compartments of increasingly smaller size until the thresholds did not change by more than 1%. Similarly, time increments were used which produced thresholds which were less than 1% different from smaller time increments. Typically, 1-μm segments and 25-μs time steps were used.

2) Cell Membrane Models: To ensure fine numerical solutions, the ganglion cell was modeled with more than 9000 compartments. Each compartment is modeled with an intracellular resistance (R_a) and a membrane mechanism in parallel with a membrane capacitance. Three membrane mechanism models were applied: a linear passive model, a Hodgkin–Huxley model with passive dendrites (HH), and an all active model (FCM) with five nonlinear ion channels distributed at varying densities.

The linear passive mechanism reduces each patch of membrane to a simple parallel RC circuit with a leak. As previously stated, the values used for membrane capacitance and resistance were 1 μF/cm^2 and 50 000 Ωcm^2, respectively. The leak conductance was modeled as a battery at -70 mV in series with a conductance of 20 μS/cm^2. This passive mechanism was present throughout the cell in all simulations. At the start of all simulations, the membrane potential everywhere was initialized to a resting potential of -70 mV.

The HH mechanism is the classic nonlinear description of unmyelinated axons by Hodgkin and Huxley [24] which is included within the simulation package NEURON—a leak conductance, sodium and potassium channels ($\overline{g}_{\rm Na} = 120$ mS/cm^2, $E_{\rm Na} = 50$ mV, $\overline{g}_{\rm K} = 36$ mS/cm^2, $E_k = -77$ mV, $\overline{g}_l = 0.3$ mS/cm^2, $E_l = -54.3$ mV). We applied the Hodgkin–Huxley channels to the soma and axon, but not the dendrites, i.e., the dendrites were passive in this model.

The FCM model is a more complex five channel model based on work by Fohlmeister *et al.* [25]–[27]. Their model includes the following conductances: $\overline{g}_{\rm Na}$ (a sodium conductance), $\overline{g}_{\rm Ca}$ (a calcium conductance), $\overline{g}_{\rm K}$ (a delayed rectifier potassium conductance), $\overline{g}_A$ (an inactivating potassium conductance), and $\overline{g}_{\rm K,\,Ca}$ (a noninactivating calcium activated potassium conductance) [25].

All channels are modeled as simple voltage-gated conductances except $\overline{g}_{\rm K,\,Ca}$, which is modeled as a calcium-gated conductance. It was this unique combination of channel kinetics which best emulated the firing pattern of ganglion cells in this species [25]. The calcium and potassium conductances served to shape the finer properties of the action potential including the ability to produce slow repetitive firing which is impossible using the Hodgkin–Huxley channels exclusively. The model for membrane potential takes the familiar Hodgkin/Huxley form [25]

$$\begin{aligned} C_m \frac{dE}{dt} = &-\overline{g}_{\rm Na} m^3 h (E - E_{\rm Na}) - \overline{g}_{\rm Ca} c^3 (E - E_{\rm Ca}) \\ &- \overline{g}_{\rm K} n^4 (E - E_K) - \overline{g}_{\rm A} a^3 h_A (E - E_K) \\ &- \overline{g}_{\rm K,\,Ca} (E - E_K) \end{aligned} \tag{1}$$

where the rate constants for m, h, c, n, a, and h_A all solve the first order kinetic equation [28]

$$\frac{dx}{dt} = -(\alpha_x + \beta_x) \cdot x + \alpha_x. \tag{2}$$

The internal calcium concentration $[{\rm Ca}]_i$ was buffered using first-order decay which can be written as

$$\frac{d[{\rm Ca}]_i}{dt} = \frac{[{\rm Ca}]_{\rm inf} - [{\rm Ca}]_i}{\tau_{\rm Ca}} \tag{3}$$

where $[{\rm Ca}]_{\rm inf}$ is the equilibrium intracellular calcium value (100 nM) and $\tau_{\rm Ca}$ is the time constant of calcium removal (1.5 ms).

These five channels were distributed with varying densities [simulated by varying the value of $g_{\max}$ (mS/cm^2) for each channel]. The densities used were identical to those proposed

TABLE I
FCM MODEL CHANNEL DENSITIES AT SOMA, DENDRITE, AND AXON (% TOTAL AXON LENGTH FROM SOMA) IN ms/cm^2

G_{max}	Soma	Dendrite	Axon(0-3%)	Axon(3-9%)	Axon(9-100%)
g_{Na}	70 mS/cm^2	40	150	100	50
g_{Ca}	1.5	3.6	1.5	0	0
g_K	18	12	18	12	15
g_{Ka}	54	36	54	0	0
$g_{K(Ca)}$	.065	.065	.065	0	0

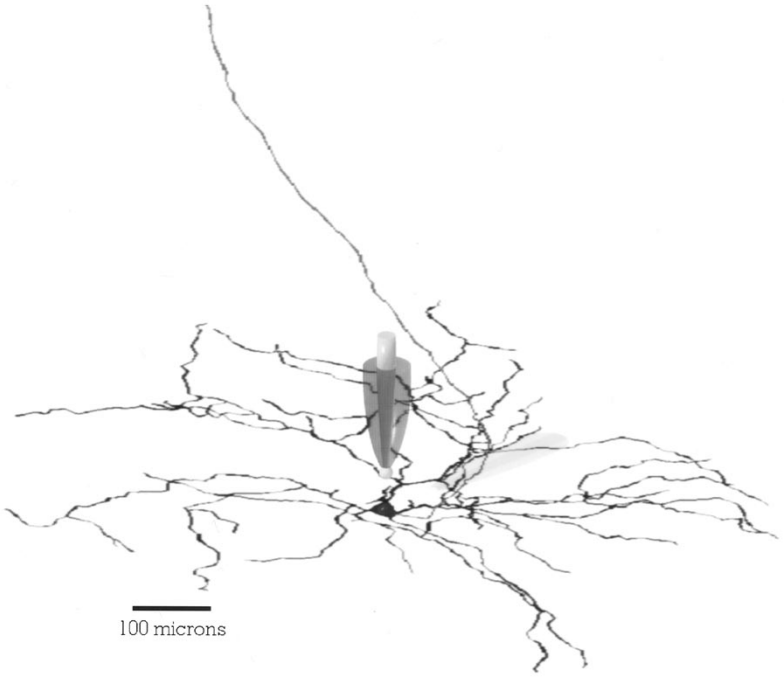

Fig. 3. A schematic illustration showing the ganglion cell being stimulated above the soma compartment from a distance of 30 μm by a spherical electrode. For a small sphere, this electrode may be modeled as an ideal point source. Scale bar = 100 μm.

by Fohlmeister *et al.* [25]–[27]. The axon was divided into three sections according to the diameter of the axon. The initial segment (0%–3% of total axon length, 0.6- to 0.8-μm diameter) of the axon starts as the axon leaves the soma and extends for approximately 30 μm. The next segment is called the "thin segment" which is narrower in diameter and continues for nearly 60 μm (3%–9% length, 0.4- to 0.6-μm diameter). The remainder of the axon (9%–100% of the approximately 1-mm length, 0.5- to 1.2-μm diameter) is fairly uniform but has a larger diameter compared to the thin segment (see Table I).

3) External Stimulus Application—Monopolar Point Source: The external medium is modeled as isopotential except when a voltage field is applied. The point electrode field was applied for 100 μs. During the application of the field, each compartment's extracellular potential is fixed based on a precomputed field for a monopolar spherical electrode in an isotropic medium [29]

$$V_e = \frac{\rho_e I}{4\pi r} \tag{4}$$

where V_e = extracellular potential, I = constant electrode current, and $\rho_e = 1/(60\Omega\text{cm})$, the resistivity of normal (0.9%) saline, which is similar to the resistivity of the vitreous humor (the biologically near-transparent liquid that occupies the intraocular cavity) [30]. We computed r as the distance between the position of the electrode and the center of each compartment. The height of the electrode was held fixed at 30 μm above the center of the soma—a distance comparable to that of the retinal ganglion cells to the internal limiting membrane (in our region of interest) [31].

Fig. 3 shows a schematic of an electrode above the ganglion cell. The electrode locations tested are shown in a top view of the neuron in Fig. 4.

4) External Stimulus Application—Disk Electrode Source: For the simulation of a disk electrode, (4) was replaced by the field from an equipotential metal disk in a semi-infinite medium, which is

$$V(r, z) = \frac{2V_o}{\pi} \sin^{-1} \left\{ \frac{2a}{[(r-a)^2 + z^2]^{1/2} + [(r+a)^2 + z^2]^{1/2}} \right\} \tag{5}$$

where (r, z) is the radial and axial distance from the center of the disk (in cylindrical coordinates) for $z \neq 0$ [32]. V_o is the potential of the disk and a is the radius of the disk. The constant voltage model of the disk electrode may be

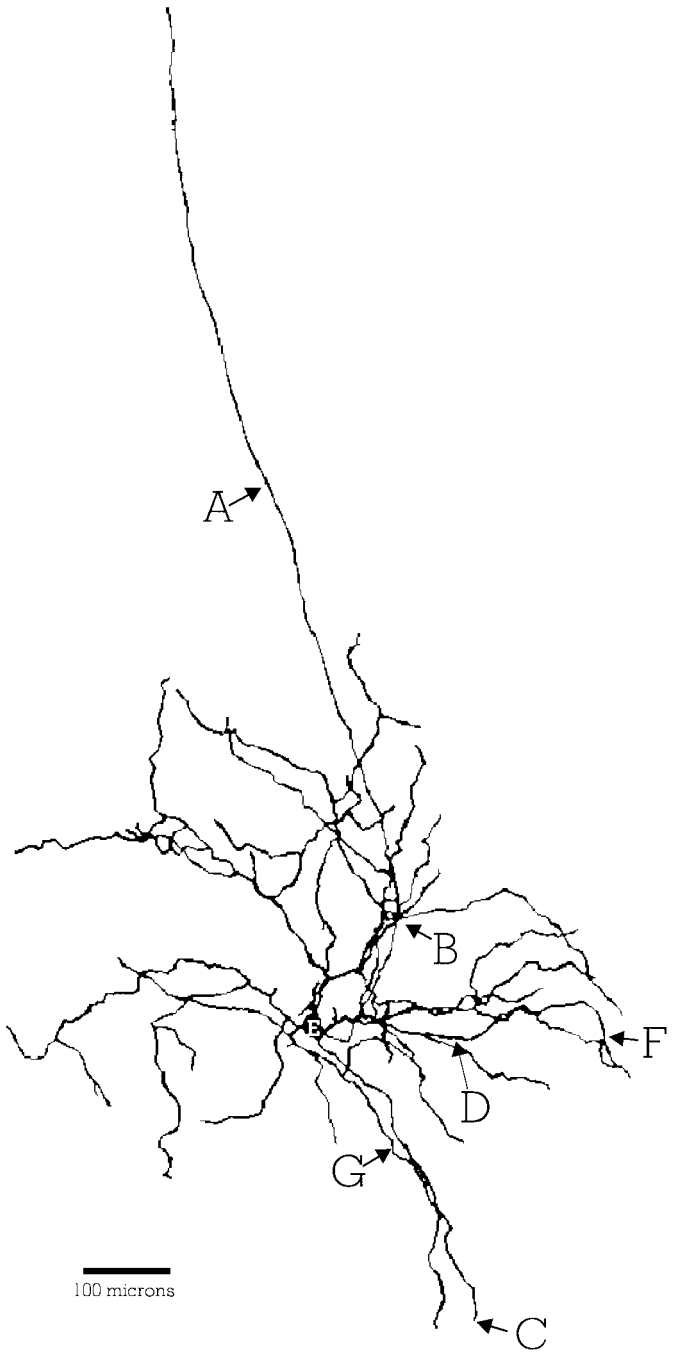

Fig. 4. A topographical view of the ganglion cell shown with its axon projecting upwards and electrode positions marked by the letters A–G. The linear distance from the soma (in μm) is: (A) over axon $\sim$503, (B) over axon $\sim$130, (C) opposite axon $\sim$334, (D) perpendicular to axon $\sim$160, (E) directly above soma, (F) perpendicular to axon $\sim$302, and (G) opposite axon $\sim$121. The vertical distance (out of the page) from electrode to the center of the nearest compartment is (in μm): (A) 33.0, (B) 30.0, (C) 34.0, (D) 30.0, (E) 30.0, (F) 29.5, and (G) 38.0.

converted to a constant current model (since the extracellular space is modeled as purely resistive) with the addition of a constant multiplicative factor. This permits comparison with the point source constant current model. Relative differences between the 50 and 100 μm disks may be directly compared. For the simulations with disk electrodes, the height was again maintained at 30 μm and the pulse duration was 100 μs.

C. Assumptions

1) Standard cable theory applies to the axon and dendrites [17], [33].
2) The electrode is modeled as an ideal point source or ideal disk. The electrical characteristics of the medium in which the current travels are linear, homogeneous and unaffected by the presence of the neuron [29]. Extracellular potentials are applied uniformly to the circumference of each cylindrical compartment. The potential applied is calculated by applying the field (4) or (5) at the center of the compartment.
3) During stimulation, the extracellular potential is determined only by the applied fields [15]. Following stimulation, the extracellular space is modeled as a short to ground, with the extracellular potential (V_{ext}) set to 0 (see Fig. 2). Note, the results of the simulation were identical when V_{ext} was not set to 0, but was instead allowed to float after the application of the stimulus.

III. Results

A. Results for Passive Model

These simulations were performed with point source electrodes, the passive membrane model and a 24-μm-diameter soma with threshold defined as 15–mV depolarization under the electrode. The absolute current required for threshold at the soma was -32.9 μA for electrode E. The absolute values predicted by this model have not been tested physiologically, so are most useful in comparing simulations [13]. Relative thresholds normalized to the current on electrode $\mathbf{E}$ are listed in Table II, column A for the passive model.

In this group of data, an electrode over the soma does not have the lowest threshold. It is easier to depolarize the membrane under many other locations other than directly over the soma due to the higher input resistances found in the smaller structures. Specifically, it is slightly easier to depolarize the axon (electrode $\mathbf{A}$) to our 15 mV threshold value. Note that these results assume only a passive membrane and are therefore highly influenced by the local input resistance.

B. Effect of Varying Electrode Position in the HH Active Model

The next group of simulations were performed with point source electrodes, the HH membrane model and a 24-μm diameter soma. The absolute current required to elicit an action potential which propagated down the axon with electrode $\mathbf{E}$ (soma) was 43-μA cathodic. The thresholds have been normalized to this current and are listed in Table II, column B for all stimulus locations.

Although the lowest threshold is found over the soma in this case, we should also note that the map of the threshold some distance from the soma is not uniform. The thresholds increase rapidly when moving further away from the soma from $\mathbf{E} \rightarrow \mathbf{D} \rightarrow \mathbf{F}$ or $\mathbf{E} \rightarrow \mathbf{G} \rightarrow \mathbf{C}$. But, if one moves along the axon $\mathbf{E} \rightarrow \mathbf{B} \rightarrow \mathbf{A}$, the threshold stays constant within a factor of two (Fig. 4)—demonstrating a relatively low axon threshold compared to the dendrites.

TABLE II
NORMALIZED CATHODIC CURRENT THRESHOLDS FOR POINT SOURCE STIMULATION WITH A 24-μm DIAMETER SOMA

Electrode	A. Relative Threshold Passive Model	B. Relative Threshold Active HH Model	C. Relative Threshold Active FCM Model
A (axon)	0.900	1.58	1.73
B	1.00	1.79	1.97
C	0.954	75.1	55.2
D	0.699	14.4	2.72
E (soma)	1.00	1.00	1.00
F	0.812	65.1	2.80
G	1.05	9.58	2.63

For all electrode locations and polarities except at **A**, the action potential at threshold was initiated 55–190 μm down the axon (the initial segment of the axon). This is consistent with the finding by Carras *et al.* that the action potential of the amphibian retinal ganglion cell is initiated in the initial segment of the axon [34]. Prior to generation of an action potential, the soma was usually depolarized, but the soma itself did not spike with the HH membrane model.

Electrode **A** produced two depolarizations when stimulating with a cathodic electrode at threshold. These depolarizations first crossed zero potential at 503 and 666 μm down the axon. These two action potentials propagated toward the soma and the terminal end of the axon, respectively.

The results produced by electrode **A** are similar to simulations of isolated axons performed by others [13], [23]. For all electrodes, the axon first crossed the zero potential from 0.8–1.5 ms after the stimulus ended.

C. Effect of Varying Electrode Position in the FCM Active Model

Next we examined the effect of different channel densities which represent a combination of channels that best emulates the spiking behavior in this species as proposed by Fohlmeister *et al.* [25]–[27]. These simulations were performed with point source electrodes, the FCM membrane model and a 24-μm diameter soma. The absolute current required to elicit an action potential with electrode **E** (soma) was 71 μA. The thresholds have been normalized to this current and are listed in Table II, column C.

The simulations with the FCM membrane model produced action potentials similar in shape to the HH model simulations and usually began in the early part of the axon (25–225 μm down the axon) except for stimulation by electrode **F**, which began at 435 μm for cathodic stimulation. The action potentials occurred 0.5–1.2 ms after the termination of the stimulus. One major difference between the HH and FCM model is that the dendrites fired action potentials in the FCM model. In fact, with the electrodes over the dendrites, an action potential was produced first in the dendrites when stimulated by an overlying electrode. This action potential was propagated to the soma. If the current was high enough to fire several dendrites simultaneously, then the action potentials summed at the soma and caused the soma to fire an action potential. Following the soma firing an action potential in this model, action potentials then propagated down the axon and retrogradely back into the dendrites.

For electrodes **C** and **G**, the dendritic action potentials were sufficient to propagate through the soma and propagate an action potential down the axon at threshold current levels. Electrodes **D** and **F** produced dendritic action potentials at low current levels, but these did not meet our criteria for "threshold" since the action potential did not propagate down the axon. The action potentials from electrodes **D** and **F** at low current levels failed at the soma and were not transmitted down the axon. The reported current thresholds for electrodes **D** and **F** are for the minimum current which caused an action potential to propagate down the axon. At this higher current level, the threshold action potential for electrodes **D** and **F** began in the early part of the axon and not at the dendrites as with electrodes **C** and **G**.

D. Effect of Replacing Point Source with a Disk Electrode

Point electrodes are an ideal representation whose closest physical analog is small spherical electrode. A practical retinal prosthesis, however, will probably not have point electrodes, but will perhaps have disks, because of limitations in microminiature manufacturing technology. Flat electrodes are easy to produce using photolithographic techniques. In fact, our monopolar clinical trials were performed with disk electrodes.

To test the effect of disk electrodes, the following simulations were performed with 50-μm-diameter disks and the HH membrane model. The cathodic threshold was 1.2 times higher over the axon (electrode **A**) compared to over the soma (electrode **E**).

Since our clinical trial also used 100-μm-diameter electrodes, we also stimulated our model cell (24-μm-diameter soma) with a 100-μm-diameter disk electrode at position **E** (over the soma). The cathodic voltage threshold was the same as for the 50-μm–diameter disk. So, cathodic disk stimuli have lower thresholds over the soma compared to over the axon by 20%.

E. Effect of Varying Soma Size in the HH Model

Although the cell that was traced had a 24-μm-diameter soma, primate somas are usually smaller than this. So, we decided to examine the effect of a smaller soma. These simulations were performed with point source electrodes, the HH membrane model and a 10-μm-diameter soma. The absolute current required to elicit an action potential in electrode **E**

(soma) was 76 μA. All thresholds were normalized to this current and were as follows: 0.895 ($\mathbf{A = axon}$), 1.03 ($\mathbf{B}$), 41.2 ($\mathbf{C}$), 8.67 ($\mathbf{D}$), 1.00 ($\mathbf{E = soma}$), 39.2 ($\mathbf{F}$), and 5.29 ($\mathbf{G}$).

The trends demonstrated by these thresholds are similar to those in Table II-B. The thresholds increase when moving further away from the soma from $\mathbf{E \rightarrow D \rightarrow F}$ or $\mathbf{E \rightarrow G \rightarrow C}$. But, if one moves along the axon $\mathbf{E \rightarrow B \rightarrow A}$, the threshold stays roughly constant. Unlike the 24-μm-diameter soma data in Table II-B, however, it is actually easier to stimulate this 10-μm-diameter soma cell with the electrode over the axon compared with the electrode over the soma.

IV. Discussion

To understand how focal electrical stimulation of retinal ganglion cells might be possible, we have studied a compartmental model of an amphibian RGC with both passive and active membrane properties and realistic geometry. We have applied extracellular electrical current both from ideal monopolar point sources and ideal disk electrodes.

A. Monopolar Point Source Electrodes—Passive Model

The passive data in Table II-A does not demonstrate a significant difference between the threshold for an electrode over the soma versus the threshold for an electrode over the axon. So, based on this simple model, we might not expect cell bodies to be preferentially stimulated compared to other regions of the cell. In fact, in these simulations, the soma seems to be one of the more difficult elements to stimulate.

Normally, a passive 1-μm structure (the size of an RGC axon) is more difficult to stimulate than a 10-μm structure (the size of an RGC soma). However, a 1-μm structure could be easier to stimulate compared to a 10-μm structure under certain circumstances. One possible explanation is that the input resistance of the smaller axon structure will be greater so that current applied to the smaller compartment will result in a larger voltage change compared to the soma which usually has a large electrical load associated with it. Moore *et al.* [36] suggest that the threshold voltage for initiating an action potential in a segment is higher if an electrical load is placed on the segment. Second, since our stimulation pulse is relatively short (100 μs), the larger capacitance observed at the soma will undoubtedly greatly filter this transient. The 1-μm axon also lies above the ganglion cell and is therefore closer to the stimulating electrode. So, location, differential loading, capacitive filtering, and the fact that smaller structures have inherently higher input resistances may account for the observation that the smaller structure is easier to stimulate than the larger structure.

These explanations apply to passive simulations and ignore the fact that ganglion cells use action potentials to propagate their signals to the brain. Since ganglion cells fire action potentials and are not passive in all regions of the cell, an active model should represent the cell more accurately.

B. Monopolar Point Source Electrodes—Active Models

With active membrane models and a 24-μm-diameter soma, the threshold over the soma is lower than over the axon. As seen in Table II-B and -C, cathodic point electrode models coupled with an active membrane (HH and FCM) demonstrate a 58%–73% increase in current required to stimulate the axon compared to the soma. So, it may be possible to electrically stimulate preferentially RGC's near their cell body at lower thresholds than at their axon when using small electrodes. This idea is consistent with our clinical observations of focal perceptions when RP patients are stimulated intraocularly [1]. It also is in agreement with animal experiments done in our lab and by others which demonstrate the ability to stimulate the retina focally [37], [38]. However, these computational results further suggest that the difference in threshold between soma and axon is likely to be less than a factor of two or even nonexistent with a smaller 10-μm-diameter soma.

The HH model in Table II-B shows a rapid increase when moving further away from the soma from $\mathbf{E \rightarrow D \rightarrow F}$ or $\mathbf{E \rightarrow G \rightarrow C}$. But, if one moves along the axon $\mathbf{E \rightarrow B \rightarrow A}$, the threshold stays roughly constant within a factor of two. This geometric asymmetry of the current threshold was not observed experimentally in the normal rabbit retina [38]. In normal rabbit, Wyatt *et al.* described a threshold which rose uniformly in all directions which may indicate excitation of cell type other than the retinal ganglion cell [38].

The HH model with passive dendrites had a threshold which rose rapidly as the electrode was moved further away from the soma. In the FCM model, there is a rapid increase when moving further away from the soma from $\mathbf{E \rightarrow G \rightarrow C}$. In Table II-C, one can see that this trend is not observed when moving from $\mathbf{E \rightarrow D \rightarrow F}$ or $\mathbf{E \rightarrow B \rightarrow A}$. It appears that the FCM model is influenced more by the physical density of the dendritic structures than the HH model. This is logical since the FCM model includes active dendrites which may fire action potentials.

Many believe that a "hot spot" of high channel density in the initial segment of the axon is excited preferentially [34]. Ranck also believed that the axon is probably stimulated when electrodes are placed near the cell body [35]. Such stimulation would be close enough to the soma to produce focal phosphenes. This method of stimulation would produce results very similar to our models, which fire action potentials in this region even without the benefit of added myelination around the soma. It is interesting that the HH model without differential channel densities (no "hot spot") also initiates action potentials in this region. Clearly, geometry is a critical factor affecting the site of initiation of action potentials, which highlights the need for realistic geometry in models of extrinsic electrical stimulation.

C. Disk Electrodes

The disk electrodes decreased the preference for stimulating near the soma versus over the axon compared to the point electrodes. This decreased preference can be explained by the distribution of current from the disk electrodes. Since the current is concentrated at the edges of the disk [32], when a 50-μm-diameter electrode is directly over a 24-μm-diameter soma, more of the current is directed around the soma compared to a point electrode directly above the soma. This

shunting of current around the soma increases the threshold over the soma relative to the threshold over the axon.

It is interesting that both the 50- and 100-μm-diameter disks required the same cathodic voltage at threshold. This suggests that for a disk electrode array placed on the surface of the retina, the cathodic threshold voltage is likely to be constant over these electrode sizes. Since the constant voltage can be converted to a constant current by taking into account electrode impedance, current density is likely to be the important design parameter at these dimensions. Interestingly, absolute current threshold and not current density has been constant in our clinical trials to date. In our human trials, the current required to reach threshold did not vary when a monopolar stimulating electrode was changed from 50-μm diameter to 100 μm [1].

D. Soma Size/Relevance of the Models to Human Clinical Findings

We would have preferred to trace a human retinal ganglion cell for these simulations, but practical constraints dictated the use of an amphibian cell. In an effort to more closely simulate a human retinal ganglion cell, we performed a series of simulations with the soma size closer to what might be found in a human retina (10 μm).

When we decreased the soma diameter to 10 μm in the HH model, we find a much smaller difference between the axon and soma thresholds. In fact, we notice a reversal from the 24-μm-diameter soma case, where it is actually easier to stimulate the axon.

It is important to note, however, that in decreasing the soma size, we did not alter any other cell dimensions or parameters, so this hybrid cell is an artificial construct which does not adequately model a human RGC. However, this cell is useful in examining the effect of soma size on threshold when compared to the cell with a 24-μm-diameter soma.

A second feature of the human retina which might decrease the observed preference in the active models for stimulating near the soma is the relative height of the axon compared to the soma. In human retina, the thickness of the nerve fiber layer can vary from 20–200 μm, but is close to 30 μm in the region we conducted our clinical experiments [39]. So, if a particularly superficial axon were much closer to the electrode than a particularly deep ganglion cell body, the axon might be preferentially stimulated in our model. This effect is not too pronounced since the potential produced by the monopolar point source falls off approximately as the reciprocal of distance (4) and not distance squared. In our model cell, the axon under electrode location **A** was 3 μm above the centerline of the soma and was about 1 μm in diameter, similar in diameter to human RGC axons.

E. Implications of Active Models for Resolution of a Retinal Prosthesis

If ganglion cells are the target of our electrical stimulation, the part of the RGC which is preferentially stimulated will affect the resolution attainable by a retinal prosthesis. If the axon is stimulated, then we might expect the spatial specificity to be limited as explained in the introduction. Alternately, if dendrites are excited, then a minimum resolution of hundreds of micrometers is possible. This poor "dendritic resolution" would be caused by the overlap of the dendritic arbors of various ganglion cells. The overlap would allow all ganglion cells whose dendrites lie under the electrode to be stimulated. So, stimulation of the dendrites at threshold currents would tend to produce larger perceptions than stimulation near the ganglion cell body. These larger percepts are produced because cells from a larger patch of retina, which correspond to a larger visual space, would be excited. Still another possibility is that the soma is excited directly, which would yield a potential resolution of around 10 μm in humans. See Fig. 1 for a graphical depiction.

From our HH simulations, it appears that the axon near the soma is stimulated, which would result in a theoretical resolution of about 10 μm, the average size of the human RGC soma. As previously noted, the threshold rose quickly in all directions except the axon. In the FCM case with active dendrites, however, the threshold does not rise as rapidly over the dendrites. In fact, since the dendrites in the FCM cell fire action potentials, a cell of this type might result in a resolution of hundreds of micrometers. The soma is still preferentially stimulated in the FCM model. But, the difference in threshold from an electrode over the soma to over the dendrites is approximately threefold. This difference might not be enough to allow selective stimulation of the soma over the dendrites.

Since the best clinical resolution achieved to date is about 500 μm [1], it is impossible to distinguish between the two alternatives at the present time. However, the clinical percepts observed to date are unlikely to be caused by axon stimulation since spots of light (and not wedges) are observed. Furthermore, the dendritic channels and their densities are unknown. But, it is now possible to patch clamp the thin dendritic arbors in cultured neurons and we suspect this channel information will soon be available and should be incorporated into future models.

F. Alternative Hypotheses to Explain Clinically Observed Focal Phosphenes in RP Patients

It is possible that other retinal cells are preferentially stimulated by electrical stimulation even though ganglion cells are physically closer to the electrodes. If photoreceptor or bipolar cells were easier to electrically stimulate, they would tend to give focal responses since their processes and receptive fields have limited spread in areas outside the fovea. In fact, photoreceptors require only a 5-μV depolarization to produce a response that can be recorded in the ganglion cell [40] (making them a likely target of electrical stimulation of normal retina).

Another reason to consider other cell types is the large degree of convergence in the retina. There are more photoreceptors than bipolar cells and more bipolars than ganglion cells. So, a greater number of deeper cells (photoreceptors or bipolars) might be stimulated compared to the number of superficial cells if the stimulus affected all layers approximately equally.

Assuming ganglion cells are the target of our electrical stimulation, another possible explanation for our clinical finding

of focal stimulation could be the differential myelination of the ganglion cell. Differential myelination might enhance the effect of electrical stimulation on the early part of the axon. In fact, Stone *et al.* suggest that RGC's of the cat are differentially enveloped by Müller cells [41]. The Müller cells were shown to engulf the soma and early part of the axon—possibly exposing a section of the axon with high channel densities.

V. Summary

A passive model of extracellular stimulation of the RGC indicated that the soma is no more easily stimulated than the axon. However, our active models suggest that it may be possible to electrically stimulate retinal ganglion cells near their cell bodies with cathodic current, but that these differences are relatively small. Our active point source models predict that the difference in threshold between soma and axon is 58%–73%. When stimulating with extracellular disk electrodes, the difference (20%) may not be significant enough to allow the preferential stimulation of somas over axons and is highly dependent on the cell's geometry (ex. soma size or axon height). We have suggested several alternative explanations for the focal perceptions observed during electrical stimulation of RP patients including the preferential excitation of deeper cells such as photoreceptors or bipolar cells.

In light of our human data [1], [5] and the results presented here, it is reasonable to continue using cathodic stimulation with flat disk electrodes for the design of retinal prostheses. But, the mechanism by which this stimulation produces focal perceptions deserves further study.

Finally, we have shown that compartmental models with active channels and realistic geometry from neuronal tracings can be achieved with reasonable computing power and should be considered in the study of extrinsically applied electrical fields.

Acknowledgment

The authors would like to thank M. Hines for his help in modifying his shareware program, NEURON, to allow the application of extracellular fields. They would also like to thank L. Cartee for her critical reading of this manuscript.

References

[1] M. S. Humayun, E. de Juan, Jr., G. Dagnelie, R. J. Greenberg, R. Propst, and D. H. Phillips, "Visual perception elicited by electrical stimulation of retina in blind humans," *Arch. Ophthalmol.*, vol. 114, pp. 40–46, 1996.

[2] J. Wyatt and J. Rizzo, "Ocular implants for the blind," *IEEE Spectrum, Mag.* pp. 47–53, 1996.

[3] J. I. Perlman, A. Y. Chow, and N. S. Peachey, "Subretinal implantation of a high density microphotodiode array in the cat retina," *Invest. Ophthalmol. Vis. Sci. Suppl.*, vol. 37, no. 3, p. S961996, Abstract.

[4] W. Roush, "Envisioning an artificial retina [news]," *Sci.*, vol. 268, pp. 637–638, 1995.

[5] R. J. Greenberg, M. S. Humayun, G. Dagnelie, R. S. Rader, and E. de Juan, Jr., "Electrical stimulation of the human retina: An update," *Invest. Ophthalmol. Vis. Sci. Suppl.*, vol. 36, no. 4, p. S-2341995, Abstract.

[6] J. G. Flannery, D. B. Farber, A. C. Bird, and D. Bok, "Degenerative changes in a retina affected with autosomal dominant retinitis pigmentosa," *Invest. Ophthalmol. Vis. Sci.*, vol. 30, pp. 191–211, 1989.

[7] J. L. Stone, W. E. Barlow, M. S. Humayun, E. de Juan, Jr., and A. H. Milam, "Morphometric analysis of macular photoreceptors and ganglion cells in retinas with retinitis pigmentosa," *Arch. Ophthalmol.*, vol. 110, pp. 1634–1639, 1992.

[8] A. M. Potts, J. Inoue, and D. Buffum, "The electrically evoked response of the visual system (EER)," *Invest. Ophthalmol.*, vol. 7, pp. 269–278, 1968.

[9] Y. Miyake, K. Yanagida, and K. Yagasaki, "Visual function proximal to the photoreceptors in primary retinitis pigmentosa," *Folia Ophthalmol. Jpn.*, vol. 32, pp. 302–308, 1981.

[10] S. Kato, M. Saito, and T. Tanino, "Response of the visual system evoked by an alternating current," *Med. Biol. Eng. Comput.*, vol. 21, pp. 47–50, 1983.

[11] Anonymous, "Field defects in open-angle glaucoma," in *Clinical Glaucoma*, G. Gorin, Ed. New York: Marcel Dekker, 1977, pp. 111–123.

[12] C. B. Toris, J. L. Eiesland, and R. F. Miller, "Morphology of ganglion cells in the neotenous tiger salamander retina," *J. Comp. Neurol.*, vol. 352, pp. 535–559, 1995.

[13] B. Coburn, "Neural modeling in electrical stimulation [review]," *Crit. Rev. Biomed. Eng.*, vol. 17, pp. 133–178, 1989.

[14] J. T. Rubinstein and F. A. Spelman, "Analytical theory for extracellular electrical stimulation of nerve with focal electrodes," *Biophys. J.*, vol. 54, pp. 975–981, 1988.

[15] R. Plonsey and R. C. Barr, "Electric field stimulation of excitable tissue," *IEEE Trans. Biomed. Eng.*, vol. 42, pp. 329–336, 1995.

[16] L. Hause, "A mathematical model for transmembrane potentials secondary to extracellular fields," in *Electroanaesthesia: Biomedical and Biophysical Studies*, A. J. Sances and S. J. Larson, Eds. New York: Academic, 1975, pp. 176–200.

[17] W. Rall, "Core conductor theory and cable properties of neurons," in *Handbook of Physiology*, J. M. Brookhart and V. B. Mountcastle, Eds. Bethesda, MD: Amer. Physiological Soc., 1977, pp. 39–97.

[18] M. Hines, "NEURON—A program for simulation of nerve equations," in *Neural Systems: Analysis and Modeling*, F. Eeckman, Ed. Norwell, MA: Kluwer Academic, 1993, pp. 127–136.

[19] T. J. Velte and R. F. Miller, "Dendritic integration in ganglion cells of the mudpuppy," *Retina Visual Neurosci.*, vol. 12, pp. 165–175, 1995.

[20] J. J. Capowski and M. J. Sedivee, "Accurate computer reconstruction and graphics display of complex neurons utilizing state-of-the-art interactive techniques," *Comput. Biomed. Res.*, vol. 14, pp. 518–532, 1981.

[21] D. F. Wann, T. A. Woolsey, M. L. Dieker, and W. M. Cowan, "An on-line digital computer system for the semi-automatic analysis of Golgi-impregnated neurons," *IEEE Trans. Biomed. Eng.*, vol. 20, pp. 233–247, 1973.

[22] P. A. Coleman and R. F. Miller, "Measurement of passive membrane parameters with whole-cell recording from neurons in the intact amphibian retina," *J. Neurophysiol.*, vol. 61, pp. 218–230, 1989.

[23] F. Rattay, *Electrical Nerve Stimulation: Theory, Experiments and Applications.* New York: Springer-Verlag, 1990.

[24] A. L. Hodgkin and A. F. Huxley, "A quantitative description of membrane current and its application to conduction and excitation in nerve," *J. Physiol.*, London, U.K., vol. 117, pp. 500–544, 1952.

[25] J. F. Fohlmeister, P. A. Coleman, and R. F. Miller, "Modeling the repetitive firing of retinal ganglion cells," *Brain Res.*, vol. 510, pp. 343–345, 1990.

[26] J. F. Fohlmeister and R. F. Miller, "A comprehensive model of repetitive impulse encoding in retinal ganglion cells," *Invest. Ophthalmol. Vis. Sci. Suppl.*, vol. 36, no. 4, pp. S-9301995, Abstract.

[27] ———, "Mechanisms by which cell geometry controls repetitive impulse firing in retinal ganglion cells," *J. Neurophysiol.*, vol. 78, pp. 1948–1964, 1997.

[28] R. Plonsey and R. C. Barr, *Bioelectricity, A Quantitative Approach.* New York: Plenum, 1988, pp. 285–286.

[29] D. R. McNeal, "Analysis of a model for excitation of myelinated nerve," *IEEE Trans. Biomed. Eng.*, vol. BME-23, pp. 329–337, 1976.

[30] L. A. Geddes and L. E. Baker, "The specific resistance of biological material—A compendium of data for the biomedical engineer and physiologist," *Med. Biol. Eng.*, vol. 5, pp. 271–293, 1967.

[31] P. R. Wheater, H. G. Burkitt, and V. G. Daniels, *Functional Histology, A Text and Color Atlas.* Edinburgh, Scotland: Churchill Livingstone, 1995, pp. 318–329.

[32] J. D. Wiley and J. G. Webster, "Analysis and control of the current distribution under circular dispersive," *Electrodes IEEE Trans. Biomed. Eng.*, vol. BME-29, pp. 381–385, 1982.

[33] I. Segev, J. W. Fleshman, and R. E. Burke, "Compartmental models of complex neurons," in *Methods in Neuronal Modeling*, C. Koch and I. Segev, Eds. Cambridge, MA: MIT Press, 1989, pp. 63–96.

[34] P. L. Carras, P. A. Coleman, and R. F. Miller, "Site of action potential initiation in amphibian retinal ganglion cells," *J. Neurophysiol.*, vol. 67, pp. 292–304, 1992.

[35] J. B. Ranck, "Which elements are excited in electrical stimulation of mammalian central nervous system: A review," *Brain Res.*, vol. 98, pp. 417–440, 1975.
[36] J. W. Moore and M. Westerfield, "Action potential propagation and threshold parameters in inhomogeneous regions of squid axons," *J. Physiol.*, London, U.K., vol. 336, pp. 285–300, 1983.
[37] M. Humayun, R. Propst, E. de Juan, Jr., K. McCormick, and D. Hickingbotham, "Bipolar surface electrical stimulation of the vertebrate retina," *Arch. Ophthalmol.*, vol. 112, pp. 110–116, 1994.
[38] J. L. Wyatt, J. F. Rizzo, A. Grumet, D. Edell, and R. J. Jensen, "Development of a silicon retinal implant: Epiretinal stimulation of retinal ganglion cells in the rabbit," *Invest. Ophthalmol. Vis. Sci. Suppl.*, vol. 35, no. 4, p. 593, 1994, Abstract.
[39] R. N. Weinreb, A. W. Dreher, A. Coleman, H. Quigley, B. Shaw, and K. Reiter, "Histopathalogic validation of Fourier-ellipsometry measurements of retinal nerve fiber layer thickness," *Arch. Ophthalmol.*, vol. 108, pp. 557–560, 1990.
[40] J. E. Dowling, *The Retina, An Approachable Part of the Brain.* Cambridge, MA: Harvard Univ. Press, 1987, pp. 131–132.
[41] J. Stone, F. Makarov, and H. Holländer, "The glial ensheathment of the soma and axon hillock of retinal ganglion cells," *Visual Neurosci.*, vol. 12, pp. 273–279, 1995.

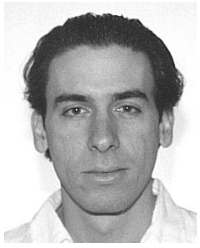

Robert J. Greenberg (S'80–M'98) was born in New York, in 1968. He received a degree in technical electronics from Nassau Technical Institute, Westbury, NY, in 1985. In 1990, he received the B.S.E. degree in electrical and biomedical engineering *summa cum laude* with honors from Duke University, Durham, NC. In 1998, he received the Ph.D. degree in biomedical engineering from the Johns Hopkins School of Medicine, Baltimore, MD. In that same year, he received the M.D. degree from the Johns Hopkins School of Medicine.

Since 1985, he has started several small companies including Campus Security, where he designed, manufactured, and marketed an electronic security system called TELEKEY®. From 1997 to 1998, he worked at the Food and Drug Administration (FDA) in the Office of Device Evaluation as a Medical Officer and was Lead Reviewer for IDE's and 510(k)'s. He is currently employed by the Alfred E. Mann Foundation for Scientific Research in Sylmar, CA. He is also Adjunct Assistant Professor in the Department of Electrical Engineering at the University of California, Los Angeles.

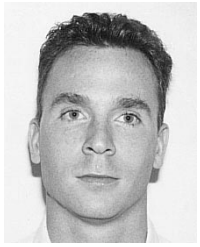

Toby J. Velte received the Ph.D. degree in neuroscience from the University of Minnesota, Minneapolis, in 1995.

He was a Research Fellow in the Department of Neurosurgery at Harvard Medical School, Cambridge, MA, until 1997. He has written numerous articles and a book about computer networks. Currently, he is CEO of a network consultancy that develops IT solutions for large companies.

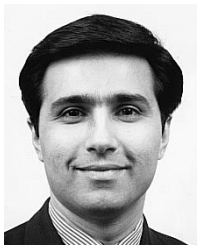

Mark S. Humayun received the M.D degree from Duke University, Durham, NC, in 1989 and the Ph.D. degree in biomedical engineering from the University of North Carolina, Chapel Hill, in 1993.

He is currently an Assistant Professor at the Wilmer Ophthalmological Institute at Johns Hopkins University, Baltimore, MD.

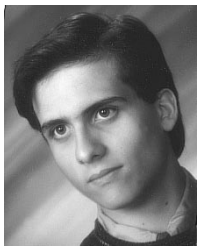

George N. Scarlatis was born in the Chicago area, IL, in 1973. He received the B.S. degree in biomedical engineering with departmental honors from Northwestern University, Evanston, IL, in 1996 and is currently pursuing the M.D. degree from Northwestern University Medical School.

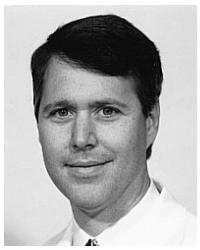

Eugene de Juan, Jr. received the Masters degree in biochemistry from the University of Alabama, Birmingham, in 1976 and the M.D. degree from the University of South Alabama College of Medicine, Mobile, in 1979.

He is currently a Professor of Ophthalmology and Co-Director of the Vitreo-Retinal Service at the Wilmer Ophthalmological Institute at Johns Hopkins University, Baltimore, MD.